AD A115788

Department of Physics and Astronomy-

THE UNIVERSITY OF IOWA

Iowa City, Iowa   52242

82   082

High Latitude Electromagnetic
Plasma Wave Emissions

by

Donald A. Gurnett

SECURITY CLASSIFICATION OF THIS PAGE (When Data Entered)

REPORT DOCUMENTATION PAGE		READ INSTRUCTIONS BEFORE COMPLETING FORM
1. REPORT NUMBER U. of Iowa 82-9	2. GOVT ACCESSION NO. *A115788*	3. RECIPIENT'S CATALOG NUMBER
4. TITLE (and Subtitle) High Latitude Electromagnetic Plasma Wave Emissions		5. TYPE OF REPORT & PERIOD COVERED Progress, May, 1982
		6. PERFORMING ORG. REPORT NUMBER
7. AUTHOR(s) Donald A. Gurnett		8. CONTRACT OR GRANT NUMBER(s) N00014-76-C-0016
9. PERFORMING ORGANIZATION NAME AND ADDRESS Dept. of Physics and Astronomy The University of Iowa Iowa City, IA 52242		10. PROGRAM ELEMENT, PROJECT, TASK AREA & WORK UNIT NUMBERS
11. CONTROLLING OFFICE NAME AND ADDRESS Electronics Program Office Office of Naval research Arlington, VA 22217		12. REPORT DATE May, 1982
		13. NUMBER OF PAGES 48
14. MONITORING AGENCY NAME & ADDRESS(If different from Controlling Office)		15. SECURITY CLASS. (of this report) UNCLASSIFIED
		15a. DECLASSIFICATION/DOWNGRADING SCHEDULE

16. DISTRIBUTION STATEMENT (of this Report)

Approved for public release; distribution is unlimited.

17. DISTRIBUTION STATEMENT (of the abstract entered in Block 20, if different from Report)

18. SUPPLEMENTARY NOTES

To be published in proceedings of the High Latitude Space Plasma Physics Nobel Symposium held in Kiruna, Sweden, March 22-25, 1982.

19. KEY WORDS (Continue on reverse side if necessary and identify by block number)

Plasma Waves
Auroral Kilometric Radiation
Auroral Hiss

20. ABSTRACT (Continue on reverse side if necessary and identify by block number)

(See page following)

DD FORM 1473 1 JAN 73   EDITION OF 1 NOV 65 IS OBSOLETE
S/N 0102-LF-014-6601

2

DTIC
COPY
INSPECTED
3

ABSTRACT

ц

This paper reviews the principal types of electromagnetic plasma

wave emissions produced in the high latitude auroral regions. Three

types of radiation are described: auroral kilometric radiation, auro-

ral hiss, and Z-mode radiation. Auroral kilometric radiation is a very

intense radio emission generated in the free space R-X mode by elec-

trons associated with the formation of discrete auroral arcs in the

local evening. Current theories suggest that this radiation is an

electron cyclotron resonance instability driven by an enhanced loss

cone in the auroral acceleration region at altitudes of about 1 to 2

R_E. Auroral hiss is a somewhat weaker whistler-mode emission

generated by low energy (100 eV to 10 keV) auroral electrons. The

auroral hiss usually has a V-shaped frequency-time spectrum caused by a

frequency dependent beaming of the whistler mode into a conical beam

directed upward or downward along the magnetic field. Ray path studies

indicate that the auroral hiss is generated in the same general region

as the auroral kilometric radiation, at altitudes of several R_E along

the auroral field lines. Z-mode radiation is a recently discovered

broadband emission similar in some respects to auroral hiss, except

that this radiation is propagating in the Z-mode. The Z-mode radiation

is trapped in the magnetosphere at frequencies between the $f_{L=0}$ cutoff

and the upper hybrid resonance, and propagates over a large region of

the polar cap in regions where the plasma frequency is well below the

gyrofrequency. Both the auroral hiss and Z-mode radiation are believed to be produced by Landau resonant interactions with low energy auroral electron beams.

INTRODUCTION

It has been known for many years that several types of electromagnetic plasma wave emissions are generated in the Earth's polar regions in association with auroras. As long ago as 1933, Burton and Boardman (1933) detected bursts of very-low-frequency (VLF) "static" at high latitudes that occurred simultaneously with flashes of auroral light. Later a variety of investigations using ground VLF radio receivers at high latitudes firmly established that broadband bursts of radio noise are produced in the auroral regions during periods of enhanced auroral activity (Ellis, 1957; Martin et al., 1960; Jorgensen and Ungstrup, 1962; Harang and Larsen, 1964). This type of VLF radio emission came to be known as "auroral hiss," following the classification scheme of Helliwell (1965). Because of the low frequencies involved, it was realized relatively early that the auroral hiss must be propagating in the whistler mode. The first satellite investigation of auroral hiss was reported by Gurnett (1966) who showed that auroral hiss is closely correlated with intense fluxes of precipitating auroral electrons. This relationship was subsequently confirmed and refined by a number of low-altitude satellite studies.

The next major advance in the study of auroral plasma wave emissions occurred when low frequency radio measurements became available from satellites in orbits extending far out from the Earth. These spacecraft were able for the first time to detect radio emissions generated above

the ionosphere, in frequency ranges which cannot propagate to the ground or to low-altitude satellites. The first evidence of radio emissions escaping from the Earth's magnetosphere was obtained from the Elektron 2 and 4 satellites by Benediktov et al., (1965), who showed that bursts of noise were observed far from the Earth at frequencies of 725 kHz and 2.3 MHz in close association with geomagnetic storms. Shortly thereafter Dunckel et al. (1970) reported similar bursts of noise at frequencies below 100 kHz, also associated with magnetic disturbances. Further reports of the spectrum of this noise were given by Stone (1973) and Brown (1973). It was not until a more extensive study by Gurnett (1974) that it was clearly established that this radio emission, which has come to be called auroral kilometric radiation, was generated at high altitudes over the auroral regions in association with bright auroral arcs. Gurnett (1974) also shows that the total power emitted by the auroral kilometric radiation is very large, up to 10^9 watts, which makes this radio emission process by far the most powerful in the Earth's magnetosphere, and comparable in many respects to other intense planetary radio sources such as Jupiter and Saturn.

In this paper we will review the principal types of electromagnetic plasma wave emissions produced in the high latitude auroral regions, with the main emphasis on recent developments and theoretical understanding. Although satellite measurements of auroral plasma wave emissions have now been available for nearly two decades, the past few years have been a period during which very rapid advances have been made. These advances involve a number of factors. Only recently, for example, have measurements been available in the critical altitude range from about 1 to 3 R_E where the most intense auroral radio emissions are being generated.

These in situ measurements now allow us to conduct detailed comparisons with theory to an extent that was not previously possible. Furthermore, in the past few years rapid advances have been made in the theoretical understanding of the plasma instabilities involved, so that there is now a framework of theoretical ideas to be compared with the experimental data. We will attempt to review all of these recent developments, concentrating particularly on electromagnetic emissions at high frequencies, where ion effects are usually not important.

MODES OF PROPAGATION

To organize the discussion of the various types of auroral electro-
magnetic emissions it is useful to briefly review the types of plasma
wave modes that can occur in the polar ionosphere. As discussed by Stix
(1962) cold plasma theory leads to the identification of four distinct
electromagnetic modes of propagation at frequencies above the ion gyro-
frequency. These modes are the free space L-O mode (left-hand polarized,
ordinary mode), the free space R-X mode (right-hand polarized, extra-
ordinary mode), the whistler mode and the Z-mode. The two free space
modes are the low frequency limits of the two free space electromagnetic
modes. The whistler-mode is named after the well-known lightning gener-
ated signals called whistlers (Storey, 1953), and the Z-mode is named
after a feature called the Z-trace in ground ionograms (Ratcliffe, 1959).
Although other modes can arise from hot plasma effects, for our purposes
it is sufficient to limit the discussion to the above four modes.

The frequency range of the four cold plasma modes is summarized in
Figure 1 for a typical electron density profile over the polar region.
The low-frequency cutoff of the free space L-O mode is at the electron
plasma frequency, f_p, which is completely determined by the electron
density, $f_p = 9\sqrt{n_e}$ kHz, where n_e is in cm^{-3}. The low-frequency cutoff
of the free space R-X mode is at a frequency called the R = 0 cutoff,
$f_{R=0} = f_g/2 + \sqrt{(f_g/2)^2 + f_p^2}$, where f_g is the electron gyrofrequency.

The whistler-mode is confined to frequencies below either f_p or f_g, whichever is smaller. The Z-mode is bounded by the upper hybrid resonance, $f_{UHR} = \sqrt{f_g^2 + f_p^2}$ and the L=0 cutoff, $f_{L=0} = -f_g/2 + \sqrt{(f_g/2)^2 + f_p^2}$.

Because f_p and f_g normally decrease with increasing radial distance, the two free space modes can escape freely from the magnetosphere. However, these modes cannot reach the ground except for frequencies above the maximum plasma frequency in the ionosphere, which is usually several MHz. As can be seen from Figure 1, neither the whistler mode nor the Z-mode can escape outward from the magnetosphere. The whistler-mode can propagate to the ground, however, the Z-mode cannot reach the ground except for a very narrow band of frequencies near the base of the ionosphere.

In the discussion that follows we will group the emission phenomena according to the mode of propagation, starting with the two free space modes, then the whistler mode, and finally the Z-mode.

AURORAL KILOMETRIC RADIATION

A typical frequency-time spectrogram of auroral kilometric radiation
is shown in Figure 2. This example was obtained from a recent DE-1 pass
over the auroral zone at an altitude of about 2 to 3 R_E. As illustrated
by this example, the kilometric radiation usually consists of a very
intense band of emission in the frequency range from about 50 to 400 kHz.
The intensity of the kilometric radiation is highly variable, often
changing by as much as 60 to 80 db on time scales of ten minutes or less.
At maximum intensity the total power radiated from the Earth (based on a
~ 2π solid angle for the emission) can be as high as 10^9 watts, although
a more typical average value is about 10^7 to 10^8 watts (Gurnett, 1974;
Kaiser and Alexander, 1977). The periods of high intensity tend to occur
in "storms" lasting from a fraction of an hour to days. Occasionally,
periods occur when no radiation at all can be detected, even down to the
limit imposed by the cosmic noise background. As shown by Gurnett (1974)
the periods of high intensity are closely correlated with global auroral
displays, particularly with discrete auroral arcs in the evening sector.
An example of the type of correlation observed is illustrated in Figure
3, which shows the radio emission intensity monitored far from the Earth
by the IMP-6 spacecraft, and a corresponding series of DMSP photographs
of the aurora taken over the northern polar region. As can be seen, the
bursts of intense kilometric radiation for DMSP orbits 1094 and 1096
occur during auroral substorms, when bright discrete auroral arcs are

present in the evening sector. Because of the close association with discrete auroral arcs, Gurnett (1974) suggested that the radiation was associated with inverted-V electron precipitation bands detected by low altitude satellites (Frank and Ackerson, 1971), which were known to cause discrete auroral arcs. This relationship has now been confirmed by direct in situ measurements in the auroral regions (Benson and Calvert, 1979; Green et al., 1979).

Both spatial intensity surveys (Gurnett, 1974; Gallagher and Gurnett, 1979) and direction-finding studies (Kurth et al., 1975; Alexander and Kaiser, 1976), show that the kilometric radiation is generated along the auroral field lines in the local evening at radial distances from about 2 to 4 R_E. The radiation is emitted in a conical emission pattern, the axis of which is tipped away from the sun toward about 22 to 24 hours, magnetic local time, approximately as shown in Figure 4. Because the radiation escapes freely from the Earth, it must be propagating in one of the two free space modes. Several independent polarization studies provide strong evidence that the radiation is generated in the right-hand polarized R-X mode (Gurnett and Green, 1978; Kaiser et al., 1978; Benson and Calvert, 1979), including recent direct measurements of the polarization with DE-1 (Shawhan and Gurnett, 1982). The polarization of the auroral kilometric radiation is not, however, without controversy, since Oya and Morioka (1982) have recently presented evidence that the radiation is propagating in the left-hand polarized L-O mode. It is possible that the kilometric radiation may consist of a mixture of both

modes. However, the recent results of Shawhan and Gurnett (1982) strongly indicate that the dominant component is right-hand polarized.

Since the discovery of the kilometric radiation, numerous theories have been proposed to explain this very intense emission. For a recent review of the proposed theories, see Grabbe (1981). The recent polarization measurements and the apparent absence of very intense electrostatic waves in the source region, which were required by several theories, strongly restricts the possible mechanisms. In our opinion the most promising mechanism is the Doppler-shifted cyclotron radiation mechanism of Wu and Lee (1979). From very general considerations the growth rate for the right-hand polarized extraordinary mode in a hot plasma can be written

$$\gamma = \frac{\pi^2 c^2 \omega_p^2}{4\omega_g} \frac{N_h}{N_c} \int_C dv_\parallel v_\perp \left[\frac{\partial F}{\partial v_\perp} + n\cos\theta \frac{\omega}{\omega_g} \frac{v_\perp}{c} \frac{\partial F}{\partial v_\parallel} \right] \tag{1}$$

where N_h and N_c are the hot and cold electron densities, F is the distribution function of the hot electrons, and $v_\parallel$ and $v_\perp$ are the parallel and perpendicular velocities relative to the magnetic field. The integral must be evaluated along a contour in velocity space defined by the cyclotron resonance condition,

$$\omega\left(1 - v_\parallel \frac{n}{c}\cos\theta\right) = \omega_g \sqrt{1 - v^2/c^2} \tag{2}$$

where n is the index of refraction, θ is the wave normal angle with respect to the magnetic field and ω is the wave frequency. As first pointed out by Wu and Lee (1979), it is important to keep the relativistic term in Equation 2 even for low velocities. For velocities $v \ll c$ and $n \simeq 1$, it can be shown that the cyclotron resonance condition is a circle in the $v_\parallel$, $v_\perp$ plane with a center at $v_\parallel = c \cos \theta$ and a radius $v_R = c[\cos^2\theta - 2\Delta\omega/\omega_g]^{1/2}$, where $\Delta\omega = \omega - \omega_g$.

The cyclotron resonance condition given by Equation 2, together with the equation for the low frequency cutoff of the R-X mode, $f_{R=0}$, accounts in a relatively straightforward way for the bandwidth of kilometric radiation, which almost always lies in the frequency range between about 50 and 500 kHz. Because $f_{R=0}$ is always well above the electron gyrofrequency when $f_p > f_g$ (see Figure 1), the energies required to Doppler shift the wave frequency above $f_{R=0}$ becomes very large, above mc^2, whenever $f_p \gtrsim f_g$. Therefore, cyclotron resonance with low energy electrons is is only possible for $f_p \ll f_g$, in the region where $f_{R=0}$ is near f_g. A typical plot of the minimum resonance energy, $W_{\parallel Res}(Min)$, as a function of altitude is shown in Figure 5 for a representative high latitude electron density profile. As indicated, the resonance energy is sufficiently low to interact with typical auroral electron energies, $W_{Auroral}$, only between points A and B, which correspond to upper and lower limits for cyclotron resonance interactions of f_B and f_A, respectively. These upper and lower frequency limits are in good quantitative agreement with the observed upper and lower frequency limits of the kilometric radiation. The limits are mainly controlled by the points in the density profile where $f_p = f_g$. If the electron density increases, or if the auroral energies

become too low, the frequency range for cyclotron resonance interactions shrinks to zero, and emission cannot occur. Either of these two effects could explain the occasional periods when no kilometric radiation is detected. Also, the bandwidth of the kilometric radiation often appears to "pinch off" at the onset and termination of a burst. This behavior is readily explained if the frequency band for cyclotron resonance is being modulated by variations in the electron density or the auroral electron energies.

Having considered the cyclotron resonance condition, we now discuss the free energy source for the cyclotron resonance instability. Two free-energy sources can be identified in Equation 1, one corresponding to a region of positive $\partial F/\partial v_{\parallel}$, and the other corresponding to regions of positive $\partial F/\partial v_{\perp}$. The condition $\partial F/\partial v_{\parallel} > 0$ is characteristic of a beam-type distribution, and was first proposed by Melrose (1976) as the free-energy source of the kilometric radiation. The condition $\partial F/\partial v_{\perp} > 0$ is characteristic of a loss-cone distribution function, and is the basis of Wu and Lee's theory. Both types of free-energy sources occur in the auroral region. Figure 6, for example, shows an electron velocity distribution obtained at high altitudes in the evening auroral zone from S3-3 (Mizera and Fennell, 1977) during a period of intense kilometric radiation. Although both free-energy sources are available, the $\partial F/\partial v_{\perp}$ term is most important. The reason is that the resonance condition (Equation 2) only gives low, $\sim$ keV, resonance energies near $\theta = \pi/2$, which makes the Cos θ term in front of $\partial F/\partial v_{\parallel}$ small. Note also that the $v_{\perp}/c$ term is small, because for the auroral electrons $v \ll c$.

As discussed by Mizera and Fennell (1977), the loss-cone feature in the distribution function is enhanced by a parallel electric field

below the satellite which widens the angular size of the loss-cone at low energies, giving the hyperbola-shaped lines in Figure 6. Thus, the existence of a parallel electric field plays an important role in enhancing the loss-cone free energy source. The maximum growth rate for the cyclotron resonance instability is obtained by adjusting the wave normal angle θ and frequency ω to locate the resonance circle in a position which gives the largest possible positive contribution of $\partial F/\partial v_\perp$ to the integral in Equation 1. Usually this requires wave normal angles nearly perpendicular to the magnetic field, $\theta \simeq 70°$ to $80°$, and frequencies very close to the gyrofrequency, $\omega \simeq 1.05 \, \omega_g$. A specific resonance circle which gives a high growth rate is shown in Figure 6. The growth rate for this case has been calculated by Omidi and Gurnett (1982), yielding a growth length for 10 e-foldings of 190 km. This growth length is comparable to the typical north-south thickness of an inverted-V region, which indicates that the cyclotron resonance instability has a sufficiently high growth rate to explain the kilometric radiation. Similar conclusions have also been obtained by Dusenbery and Lyons [1982] and Melrose et al. [1982].

Because the maximum growth rate occurs nearly perpendicular to the magnetic field the cyclotron resonance instability has the proper emission direction required to explain the angular distribution of the radiation. For waves generated near $\theta = \pi/2$ the radiation tends to be refracted into a conical emission pattern with a half angle of $50°$ to $80°$ because of the gradient in the index of refraction near the R=0 cutoff surface (Green et al., 1979). The superposition of many such conical emission patterns along an extended east-west source qualitatively

accounts for the observed emission pattern of the kilometric radiation. The plasmapause also plays a significant role in blocking the radiation, producing a shadow zone near the equatorial plane, as indicated in Figure 4.

Although spectrograms such as in Figure 2 show an almost continuous band of emission, much higher resolution spectrograms, as in Figure 7, show that the radiation actually consists of many extremely narrowband emissions with rapidly varying center frequencies (Gurnett et al., 1979). These discrete features have a marked similarity to discrete whistler-mode emissions in the Earth's magnetosphere (Helliwell, 1965), including many effects remarkably similar to the nonlinear interactions induced in magnetospheric whistler-mode emissions by ground VLF transmitters. This close similarity is probably more than coincidental, because if Wu and Lee's mechanism is correct both types of emission involve a cyclotron resonance interaction driven by a loss-cone distribution. The only difference is that the Doppler shift is downward, below f_g, for the whistler-mode emissions, and upward, above $f_{R=0} \simeq f_g$, for the kilometric radiation.

Recently, Calvert (1982) has advanced an explanation which appears to account for many of the characteristics of the fine structure. In his model he suggests that many nearly field-aligned irregularities in the source region produce partial reflections of the perpendicularly propagating radiation, like the mirrors in a laser. The resulting feedback makes the system operate like an oscillator, with a spectrum of normal modes arising from the requirement for an integral number of wavelengths around the feedback loop. This model can account for the occasional occurrence of harmonically spaced spectral features, for example, at

about 0549 UT in Figure 7, as well as many other detailed features. The systematic variation in the emission frequency occurs because of changes in the perpendicular distance between the irregularities, which force the frequency to change, with a corresponding motion of the source region up or down the field line to maintain the emission frequency near the gyro-frequency. If this model is correct, the kilometric radiation may have many features in common with a laser.

AURORAL HISS AND SAUCERS

A typical example of an auroral hiss event observed by a low-altitude satellite is shown in Figure 8. This spectrogram identifies two types of emissions called "auroral hiss" and "saucers." Both types of emission have a characteristic V-shaped signature on a frequency-time spectrogram. Poynting flux measurements (Mosier and Gurnett, 1969) show that the two types of emission are propagating in opposite directions along the magnetic field line. The downward propagating emissions were called auroral hiss (also, VLF hiss, and V-shaped hiss), consistent with the prior use of this term for ground-based observations, and the upward propagating emissions were called saucers, following the terminology first introduced by Brice, Smith and Barrington (unpublished remarks). Because it is usually difficult without Poynting flux measurements to distinguish the upward and downward propagating emissions, the use of these various terms has become somewhat confused in the literature. Therefore, we refer to all of these emissions as auroral hiss, commenting on the upgoing or downgoing nature of the propagation only when known. Because the frequency of these emissions is well below either the electron gyrofrequency or plasma frequency, it is clear that these emissions are propagating in the whistler mode.

The V-shaped appearance of the auroral hiss spectrum for both the upgoing and downgoing waves has a simple interpretation based on the propagation of whistler-waves from a spatially localized source. Electric and magnetic field intensity comparisons show that the auroral hiss

is propagating at large wave normal angles near the resonance cone in a
regime where the whistler-mode is quasi-electrostatic. For wave normal
angles near the resonance cone it can be shown that the ray path is per-
pendicular to the resonance cone at an angle ψ_{Res} with respect to the
magnetic field, as shown in Figure 9. The angle ψ_{Res} is given by

$$\text{Tan}^2\psi_{Res} = -\frac{S}{P} \simeq \frac{f_p^2 f^2}{(f_p^2 - f^2)(f_g^2 - f^2)} \tag{3}$$

where S and P are defined by Stix (1962) and the approximation is
valid at high densities, $f_p \gtrsim f_g$, and ignores ion effects. Equation
3 shows that at low frequencies the ray path is almost exactly along
the magnetic field, and that the angle of propagation increases with
increasing frequency, approaching $\pi/2$ at the upper frequency limit of
the whistler mode, either f_p or f_g, whichever is small.. (see Figure
1). When ion effects are included ψ_{Res} goes to zero at the lower
hybrid resonance f_{LHR}.

If a satellite passes through the beam of radiation from a point
source, as illustrated in the right-hand panel of Figure 9, the high-
est frequencies are detected first, with progressively lower frequen-
cies as the spacecraft approaches the field line through the source.
The detailed shape of the radiation spectrum within the beam is
determined by the source geometry. For a point source the emission
will only be detected near the outer edges of the V-shaped feature,
as for the saucer in Figure 8, whereas for an extended line or sheet

source the V-shaped feature will be filled in. Evidence for both types of source geometries can be found in the data (Gurnett and Frank, 1972; James, 1976). The existence of a sharp cutoff at the edges of the V-shaped features indicates that the source is either sharply localized (point or horizontal line geometry) or has a sharply defined altitude limit (field-aligned sheet geometry). Rough estimates based on the shape of the V-shaped cutoff place the source of the downgoing auroral hiss at relatively high altitudes, from about 5,000 to 10,000 km (Gurnett and Frank, 1972). The source of the upgoing auroral hiss (saucers) is much lower in the ionosphere, from about 1,000 to 3,000 km (Mosier and Gurnett, 1969; James, 1976). Recently, Gurnett et al. (1982) have reported observations of upgoing auroral hiss with DE-1 at altitudes of 2 to 3 R_E over the auroral zone. The source of these upgoing emissions appears to be at altitudes of 0.7 to 0.9 R_E (4500 to 5700 km). It seems likely that DE-1 is detecting the same upgoing auroral hiss (saucer) emissions detected by low altitude satellites, although this relationship has not yet been established.

Comparisons with charged particle measurements have now firmly established that the downgoing auroral hiss is closely correlated with inverted-V electron precipitation events (Gurnett and Frank, 1972; Hoffman and Laaspere, 1972; Laaspere and Hoffman, 1976). The type of correlation observed is illustrated in Figure 8, which shows a downgoing auroral hiss event occurring almost exactly coincident with an intense inverted-V event extending up to energies of several keV. The correlation with these electron precipitation events remains good even if the electron energies are quite low, down to 100 eV or less. The downgoing

auroral hiss emissions are observed around most of the auroral oval, from the polar cusp on the dayside of the Earth, through local afternoon, and into the local evening region, very similar to the region of occurrence of inverted-V events (Frank and Ackerson, 1972). Although the downgoing auroral hiss events are clearly associated with inverted-V electron precipitation events, the upgoing auroral hiss (saucer) emissions have never been associated with any clearly identifiable feature in the charged particle data. Typically, the upgoing emissions occur near the boundaries of an electron precipitation region, as is the case for the saucer in Figure 8. This relationship has led to the idea that the up-going emissions are associated with a return current of upgoing iono-spheric electrons related to the nearby electron precipitation region. The geometry of this current system and the corresponding emission regions for the upgoing and downgoing auroral hiss are illustrated schematically in Figure 10. Because the upgoing saucer emissions at low altitude are of very short duration, sometimes lasting only seconds, the spatial thickness of the return current of upgoing ionospheric electrons must be very small, 10 km or less. Because the thickness of the return current is small and because the electron energies involved are quite low, < 5 eV, it is believed that the electrons responsible for the up-going saucer emissions simply could not be detected with the available instrumentation.

Two types of theories have been proposed to explain the auroral hiss emissions: incoherent Cerenkov radiation (Ellis, 1957; Jorgensen, 1968; Taylor and Shawhan, 1974) and coherent plasma instabilities (Maggs, 1976; James, 1976; Maggs and Lotko, 1981). Although Cerenkov radiation has

many desirable features, it is generally concluded that this mechanism cannot produce the high intensities typically observed in the auroral hiss. Of the plasma instabilities which have been considered, it is virtually certain, because of the quasi-electrostatic nature of the whistler-mode near the resonance cone, that the emission is produced by a Landau resonance at $v_\parallel = \omega/k_\parallel$, rather than by a cyclotron resonance. The instability is then driven by a region of positive $\partial F/\partial v_\parallel$ in the distribution function, characteristic of a beam. Because the Landau resonance occurs for waves propagating in the same direction as the beam, this mechanism produces downgoing emissions in the inverted-V region, in agreement with observations.

As illustrated in Figure 6, beamlike features are a common characteristic of the auroral electron distribution function and are responsible for the peak in the energy spectrum of the inverted-V events. Precipitating electron beams of this type have been modelled by Maggs and Lotko (1981). Their calculations show that whistler-mode growth occurs over a broad range of altitudes. Computed equilibrium electric field intensities appear to be in good agreement with observed auroral hiss intensities when realistic beam densities are used. The observations are therefore in reasonable agreement with theoretical predictions. The only shortcoming of the present calculations is that they are based on electron distribution functions measured by low altitude satellites. Because of the presence of parallel electric fields it is not clear how reliably the low altitude measurements can be extrapolated up to the relatively high altitude where the auroral hiss is generated.

Z-MODE RADIATION

Because of the electrostatic character of the Z-mode near the upper hybrid resonance, it has often been suggested that Z-mode emissions (also called upper hybrid emissions) should be produced by auroral electron beams. This mode has been considered for generating auroral kilometric radiation via coupling with one of the free space modes (Benson, 1975; Roux and Pellat, 1979; Oya and Morioka, 1982). Despite the theoretical interest in Z-mode emissions very little is known about these emissions in the auroral regions. Z-mode emissions have in at least two cases been reported in the auroral region with low-altitude satellites (Gregory, 1969; Hartz, 1970). Gregory (1969) describes observations of Z-mode emissions correlated with low energy auroral electrons and suggests that the emissions are produced by Cerenkov radiation. As can be seen in Figure 1, at low altitudes the Z-mode is confined to a relatively narrow frequency band around f_p.

Recently, the DE-1 spacecraft has provided the first observations of broadband Z-mode radiation in the low density region over the polar region; in the regime where the frequency band of the Z-mode is very broad (Gurnett et al., 1982). A typical example of the Z-mode radiation detected by DE-1 is shown in Figure 11. The Z-mode radiation in this case occurs in a frequency range slightly above an upgoing auroral hiss event of the type described earlier. The upper cutoff frequency of the

auroral hiss is at the local plasma frequency, f_p, as expected in the very low density region over the polar cap where $f_p < f_g$ (see Figure 1). The Z-mode emission has approximately the same intensity as the auroral hiss and has an upper frequency cutoff near the electron gyrofrequency. In the frequency range below f_g, the Z-mode is almost purely electromagnetic with an index of refraction close to one (Ratcliffe, 1959). In the altitude window between $f_{L=0}$ and f_g, the radiation propagates nearly isotropically, with refraction away from the cutoff at $f_{L=0}$, and refraction toward a contour of constant $f = f_g$ as the wave approaches f_g from below. Because of the absence of strong directional characteristics the Z-mode radiation can propagate considerable distances horizontally over the polar cap in the frequency window between $f_{L=0}$ and f_g. The long range of propagation therefore makes it difficult to clearly establish that the radiation originates from the auroral zone, although the auroral zone is probably the only reasonable source.

Because of the recent identification of the polar Z-mode radiation with DE-1 and the uncertainty about the exact source region, it is difficult to be certain just how this radiation is generated. All current theories for Z-mode emissions concentrate on the frequency range between f_g and f_{UHR}, where the Z-mode becomes quasi-electrostatic and has very low phase velocities near the resonance cone. As with the auroral hiss, two types of emission processes have been considered: incoherent Cerenkov radiation (Gregory, 1969; Taylor and Shawhan, 1974), and coherent plasma instabilities (Maggs and Lotko, 1981). In many respects the mechanisms proposed for explaining Z-mode emission are nearly identical

to those proposed for explaining auroral hiss. The only essential difference is the mode of propagation, and even here the similarities are very close, because both modes of propagation are quasi-electrostatic with wave normal angles very close to the resonance cone. Once produced in the quasi-electrostatic region between f_g and f_{UHR}, the radiation can propagate into the frequency range below f_g if suitable density gradients exist in the source region. A sketch of the resulting ray paths is shown in Figure 12, assuming an auroral source. At the present time, because of the preliminary nature of the observations, it is too soon to know if this mechanism will be able to account for all of the observed characteristics of the Z-mode emissions.

CONCLUSIONS

In this paper we have reviewed the principal types of electromagnetic plasma wave emissions observed in the Earth's polar magnetosphere. Electromagnetic emissions have been detected from the auroral regions in three of the four cold plasma modes: the free space R-X mode, the whistler-mode and the Z-mode. Electromagnetic emissions are also known to be produced in the free space L-O mode by coupling with electrostatic waves near the upper hybrid resonance (Kurth et al., 1981), however, at the present time these emissions, called continuum radiation, have not been identified with a high latitude source. Of these emissions the kilometric radiation is particularly important because very similar right-hand polarized radio emissions are known to be generated at high latitudes in the magnetospheres of Jupiter (Warwick et al., 1979) and Saturn (Kaiser et al., 1980), and possibly Uranus (Brown, 1976). Auroral hiss emissions have also been detected near the Io plasma torus at Jupiter (Gurnett et al., 1979). These diverse observations illustrate the basic importance of understanding electromagnetic emission processes in plasmas. When adequately understood it is likely that these radio emissions will provide a valuable diagnostic tool for understanding plasma processes in regions not immediately accessible to direct measurements, such as the aurora at Jupiter and Saturn. It is only by continued study of these emissions in the Earth's auroral regions that we are likely to achieve a complete understanding of the mechanisms involved.

ACKNOWLEDGEMENTS

REFERENCES

Alexander, J. K., and Kaiser, M. L., 1976, Terrestrial kilometric radiation. 1. Spatial structure studies, J. Geophys. Res., 81:5948.

Benediktov, E. A., Getmantsev, G. G., Sazonov, Yu. A., and Tarasov, A. F., 1965, Preliminary results of measurements of the intensity of distributed extraterrestrial radio-frequency emission at 725 and 1525-kHz frequencies by the satellite electron-2, Kosm. Issled., 3:614.

Benson, R. F., 1975, Source mechanism for terrestrial kilometric radiation, Geophys. Res. Lett., 2:52.

Benson, R., and Calvert, W., 1979, ISIS 1 observations at the source of auroral kilometric radiation, Geophys. Res. Lett., 6:479.

Brown, L. W., 1973, The galactic radio spectrum between 130 kHz and 2,600 kHz, Astrophys. J., 180:359.

Brown, L. W., 1976, Possible radio emission from Uranus at 0.5 MHz, Astrophys. J., 207:L202.

Burton, E. T., and Boardman, E. M., 1933, Audio-frequency atmospherics, Proc. IRE, 21:1476.

Calvert, W., 1982, A feedback model for the source of auroral kilometric radiation, J. Geophys. Res., submitted.

Dunckel, N., Ficklin, B., Rorden, L., and Helliwell, R. A., 1970, Low frequency noise observed in the distant magnetosphere with OGO 1, J. Geophys. Res., 75:1854.

Dusenbery, P. B., and L. R. Lyons, 1982, General concepts on the generation of auroral kilometric radiation, J. Geophys. Res., in press.

Ellis, G. R., 1957, Low-frequency radio emission from aurorae, J. Atmos. Terr. Phys., 10:302.

Frank, L. A., and Ackerson, K. L., 1971, Observations of charged-particle precipitation into the auroral zone, J. Geophys. Res., 76:3612.

Frank, L. A., and Ackerson, K. L., 1972, Local-time survey of plasma at low altitudes over the auroral zones, J. Geophys. Res., 77:4116.

Gallagher, D. L., and Gurnett, D. A., 1979, Auroral kilometric radiation: Time-averaged source position, J. Geophys. Res., 84:6501.

Grabbe, C. L., 1981, Auroral kilometric radiation: A theoretical review, Rev. Geophys. and Space Phys., 19:627.

Green, J. L., Gurnett, D. A., and Hoffman, R. A., 1979, A correlation between auroral kilometric radiation and inverted-V electron precipitation, J. Geophys. Res., 84:5216.

Gregory, P. C., 1969, Radio emission from auroral electrons, Nature, 221:351.

Gurnett, D. A., 1966, A satellite study of VLF hiss, J. Geophys. Res., 71:5599.

Gurnett, D. A., 1974, The earth as a radio source: Terrestrial kilometric radiation, J. Geophys. Res., 79:4227.

Gurnett, D. A., Anderson, R. R., Scarf, F. L., Fredricks, R. W., and Smith, E. J., 1979, Initial results from the ISEE-1 and -2 plasma wave investigation, Space Sci. Rev., 23:103.

Gurnett, D. A., and Frank, L. A., 1972, VLF hiss and related plasma observations in the polar magnetosphere, J. Geophys. Res., 77:172.

Gurnett, D. A., and Green, J. L., 1978, On the polarization and origin of auroral kilometric radiation, J. Geophys. Res., 83:689.

Gurnett, D. A., Kurth, W. S., and Scarf, F. L., 1979, Auroral hiss
observed by Voyager 1 near the Io plasma torus, Nature, 280:767.

Gurnett, D. A., Shawhan, S. D., and Shaw, R. R., 1982, Auroral hiss, Z-
mode radiation and auroral kilometric radiation in the polar magnet-
osphere: DE-1 observations, J. Geophys. Res., submitted.

Harang, L., and Larsen, R., 1964, Radio wave emissions in the VLF band
observed near the auroral zone. 1. Occurrence of emissions during
disturbances, J. Atmosph. Terr. Phys., 27:481.

Hartz, T. R., 1970, Low frequency noise emissions and their significance
for energetic particle processes in the polar ionosphere, in "The
Polar Ionosphere and Magnetospheric Processes," G. Skovli, ed.,
Gordon and Breach, New York.

Helliwell, R. A., 1965, "Whistlers and Related Ionospheric Phenomena,"
Stanford University Press, Stanford.

Hoffman, R. A., and Laaspere, T., 1972, Comparison of very-low-frequency
auroral hiss with precipitating low-energy electrons by the use of
simultaneous data from two OGO 4 experiments, J. Geophys. Res.,
77:640.

James, H. G., 1976, VLF saucers, J. Geophys. Res., 81:501.

Jorgensen, T. S., 1968, Interpretation of auroral hiss measured on OGO 2
and at Byrd Station in terms of incoherent Cerenkov radiation,
J. Geophys. Res., 73:1055.

Jorgensen, T. S., and Ungstrup, E., 1962, Direct observation of correla-
tion between aurorae and hiss in Greenland, Nature, 194:462.

Kaiser, M. L., and Alexander, J. K., 1977, Terrestrial kilometric radi-
ation: 3. Average spectral properties, J. Geophys. Res., 82:3273.

Kaiser, M. L., Alexander, J. K., Riddle, A. C., Pearce, J. B., and
Warwick, J. W., 1978, Direct measurements of the polarization of
terrestrial kilometric radiation from Voyagers 1 and 2, Geophys.
Res. Lett., 5:857.

Kaiser, M. L., Desch, M. D., Warwick, J. W., and Pearce, J. B., 1980,
Voyager detection of nonthermal radio emission from Saturn, Science,
209:1238.

Kurth, W. S., Baumback, M. M., and Gurnett, D. A., 1975, Direction-
finding measurements of auroral kilometric radiation, J. Geophys.
Res., 80:2764.

Kurth, W. S., Gurnett, D. A., and Anderson, R. R., 1981, Escaping
nonthermal continuum radiation, J. Geophys. Res., 86:5519.

Laaspere, T., and Hoffman, R. A., 1976, New results on the correlation
between low-energy electrons and auroral hiss, J. Geophys. Res.,
81:524.

Maggs, J. E., 1976, Coherent generation of VLF hiss, J. Geophys. Res.,
81:1707.

Maggs, J. E., and Lotko, W., 1981, Altitude dependent model of the auro-
ral beam and beam-generated electrostatic noise, J. Geophys. Res.,
86:3439.

Martin, L. H., Helliwell, R. A., and Marks, K. R., 1960, Association
between aurorae and very-low-frequency hiss observed by Byrd
Station, Antarctica, Nature, 187:751.

Melrose, D. B., 1976, An interpretation of Jupiter's decametric radiation
and terrestrial kilometric radiation as direct amplified gyroemis-
sion, Astrophys. J., 207:651.

Melrose, D. B., Ronnmark, K. G., and Hewitt, R. G., 1982, Terrestrial
kilometric radiation: The cyclotron theory, J. Geophys. Res., in
press.

Mizera, P. F., and Fennell, J. F., 1977, Signatures of electric fields
from high and low altitude particle distributions, Geophys. Res.
Lett., 4:311.

Mosier, S. R., and Gurnett, D. A., 1969, VLF measurements of the Poynting
flux along the geomagnetic field with the Injun 5 satellite,
J. Geophys. Res., 74:5675.

Omidi, N., and Gurnett, D. A., 1982, Growth rate calculations of auroral
kilometric radiation using the relativistic resonance condition,
J. Geophys. Res., in press.

Oya, H., and Morioka, A., 1982, Observational evidences of Z-mode waves
as the origin of auroral kilometric radiation based on AKR data
detected by JIKIKEN (EXOS-B) satellite, J. Geophys. Res., submit-
ted.

Ratcliffe, J. A., 1959, "The Magneto-Ionic Theory and Its Applications to
the Ionosphere," Cambridge University Press, Cambridge.

Roux, A., and Pellat, R., 1979, Coherent generation of the auroral kilo-
metric radiation by nonlinear beatings between electrostatic waves,
J. Geophys. Res., 84:5189.

Shawhan, S. D., and D. A. Gurnett, 1982, The polarization of auroral
kilometric radiation, Geophys. Res. Lett., in preparation.

Stix, T. H., "The Theory of Plasma Waves," 1962, McGraw-Hill, New York.

Stone, R. G., 1973, Radio physics of the outer solar system, Space Sci. Rev., 14:534.

Storey, L. R. P., 1953, An investigation of whistling atmospherics, Phil. Trans. Roy. Soc. London A, 246:113.

Taylor, W. W. L., and Shawhan, S. D., 1974, A test of incoherent Cerenkov radiation for VLF hiss and other magnetospheric emissions, J. Geophys. Res., 79:105.

Warwick, J. W., Pearce, J. B., Riddle, J. C., Alexander, J. K., Desch, M. D., Kaiser, M. L., Thieman, J. R., Carr, T. D., Gulkis, S., Boischot, A., Harvey, C. C., Pedersen, B. M., 1979, Voyager 1 planetary radio astronomy observations near Jupiter, Science, 204:995.

Wu, C. S., and Lee, L. C., 1979, A theory of terrestrial kilometric radiation, Astrophys. J., 230:621.

FIGURE CAPTIONS

Figure 1   Frequency range of the four cold plasma modes for

a representative electron density profile over the

polar region.

Figure 2   Frequency-time spectrogram of auroral kilometric

radiation for a high altitude DE-1 pass over the

evening auroral zone.

Figure 3   Intensity variations of auroral kilometric radi-

ation detected about 30 R_E from the Earth and a

sequence of photographs of the aurora taken over

the northern polar region.

Figure 4   Sketch of the ray paths and source region of

auroral kilometric radiation.

Figure 5   The minimum cyclotron resonance energy,

$W_{\parallel Res}(Min)$, as a function of altitude for a typi-

cal ionospheric model. Resonance can occur only

if f_p is well below f_g.

Figure 6   An inverted-V electron distribution function obtained
                by S3-3 during a kilometric radiation event.

Figure 7   High resolution spectrograms of auroral kilometric
                radiation from ISEE-1 showing the very complex fine
                structure of the kilometric radiation.

Figure 8   An example of auroral hiss and saucers obtained from a
                low altitude satellite showing the correlation with an
                inverted-V electron precipitation event.

Figure 9   Geometric constructions used to explain the V-shaped
                frequency-time spectrum of auroral hiss.

Figure 10   The source region of the saucer and auroral hiss emis-
                sions and their relationship to the inverted-V elec-
                tron precipitation region and the associated return
                current of upgoing ionospheric electrons.

Figure 11   A high altitude DE-1 pass showing an upgoing auroral
                hiss event and Z-mode radiation over the evening auro-
                ral zone.

Figure 12   Typical ray paths for the Z-mode radiation, assuming
                an auroral zone source near the upper hybrid
                resonance.

37

Figure 1

A-G82-229

POLAR CAP   AURORAL KILOMETRIC   PLASMAPAUSE
                  RADIATION
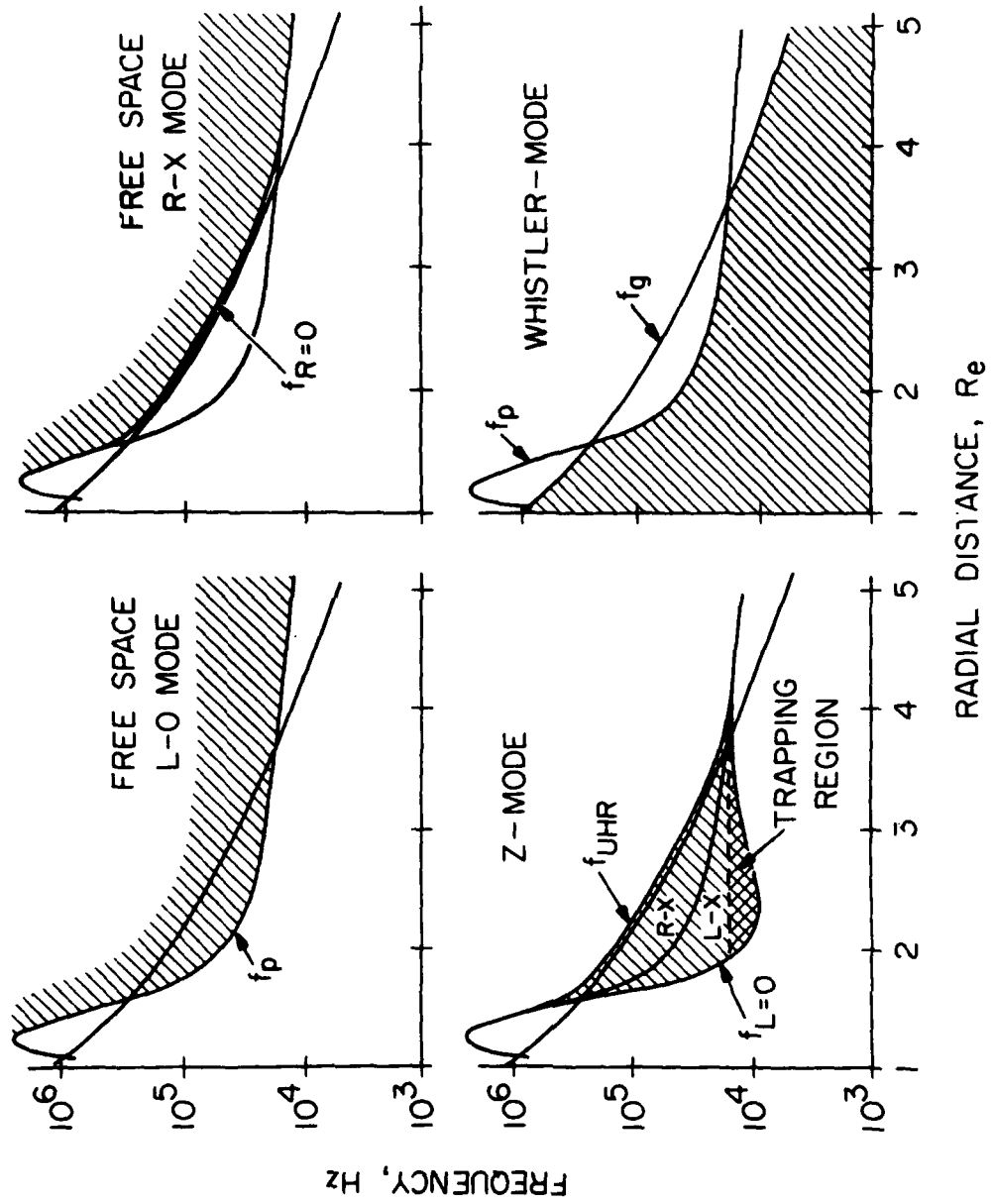
FREQUENCY kHz	400						
	100						
	40						
UT	1250	1310	1330	1350	1410	1430	
R(R$_E$)	4.5	4.3	4.1	3.7	3.3	2.8	
L			20.0	11.7	7.0	4.1	
MLT	20.9	21.4	21.7	21.9	22.1	22.1	
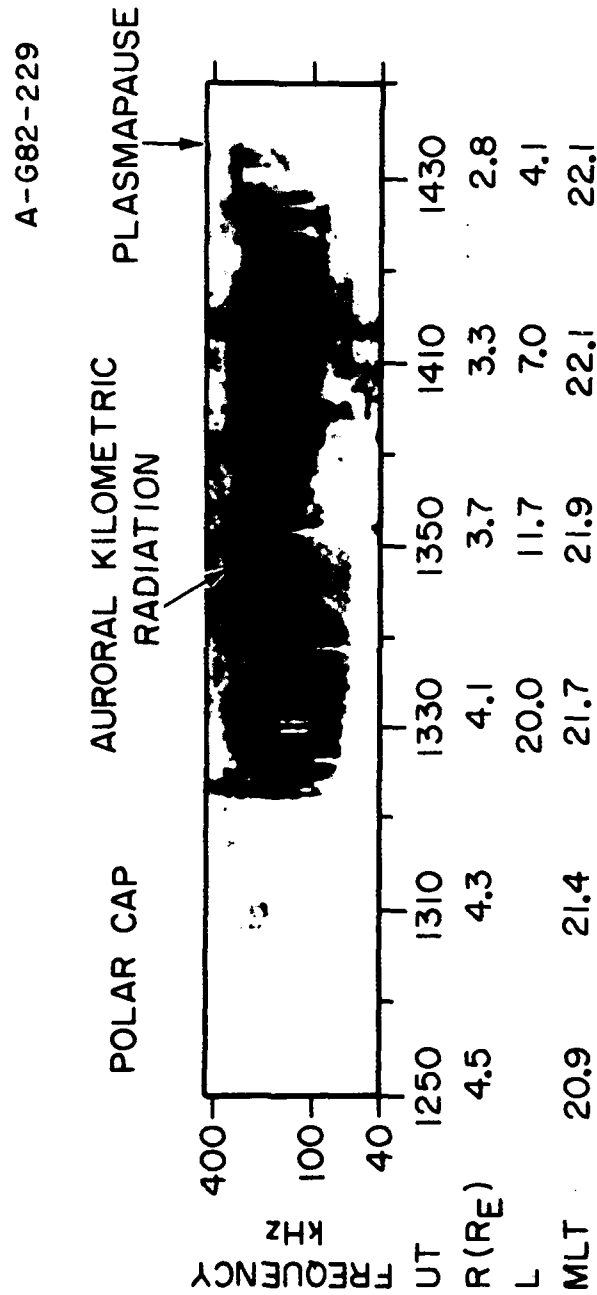
DE-1, OCTOBER 2, 1981

Figure 2

39

Figure 3

Figure 4

Figure 5

Figure 6

B-G82-231

R = 5.888 R$_E$ MAG LAT = 41.0°   MLT = 3.8 HRS

FREQUENCY (kHz)
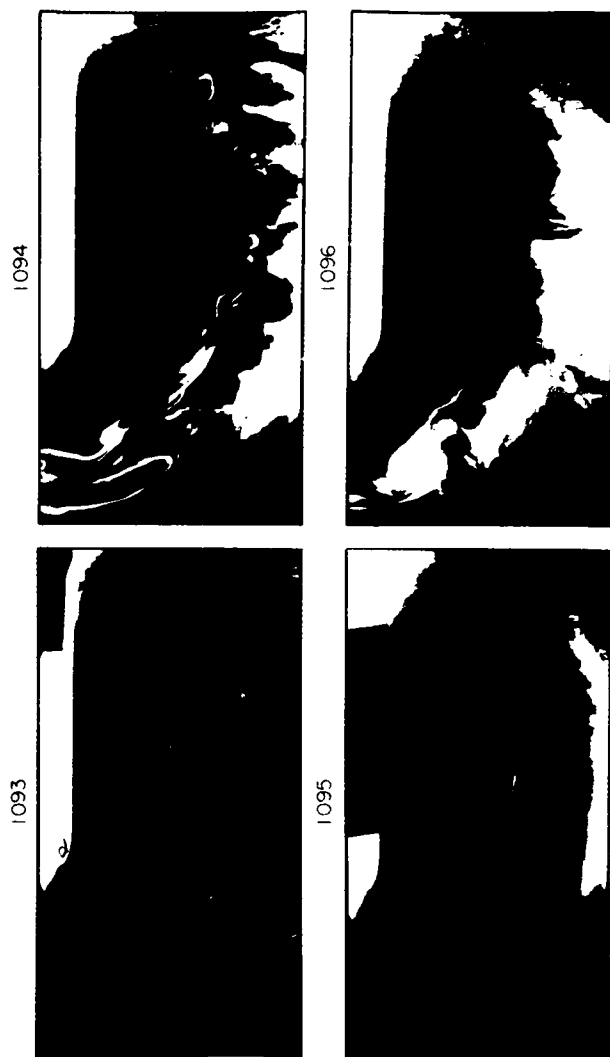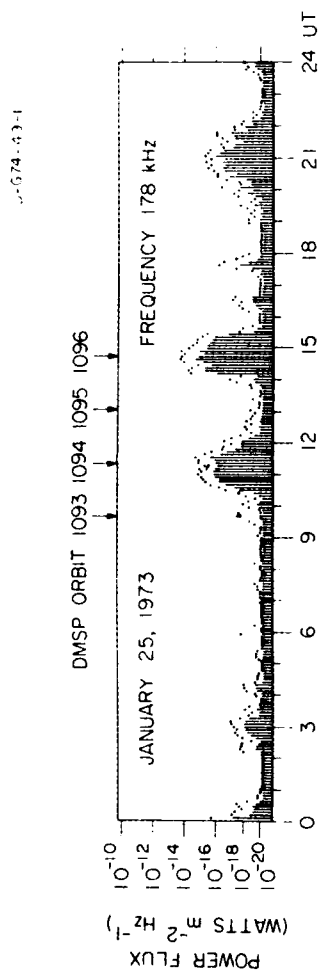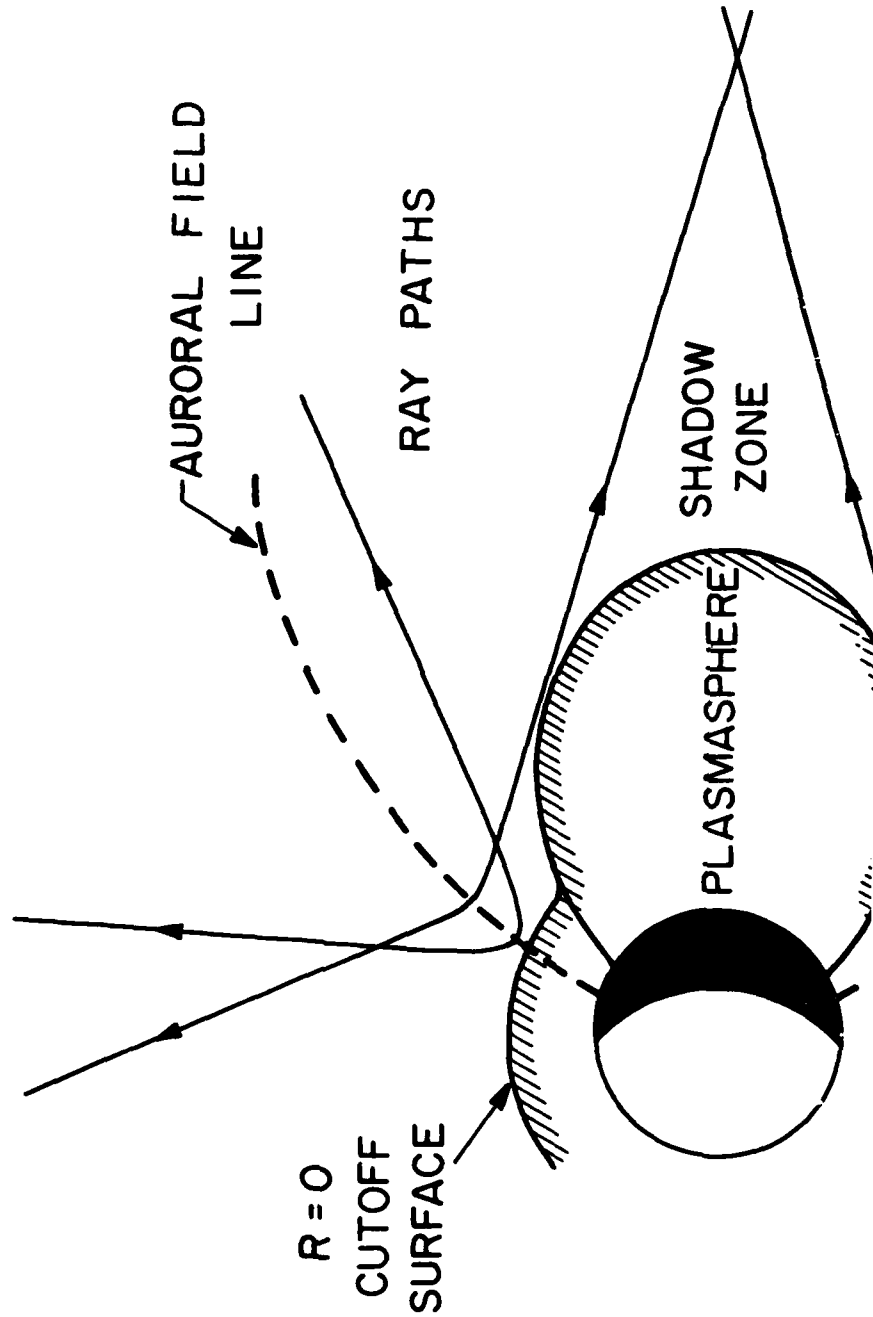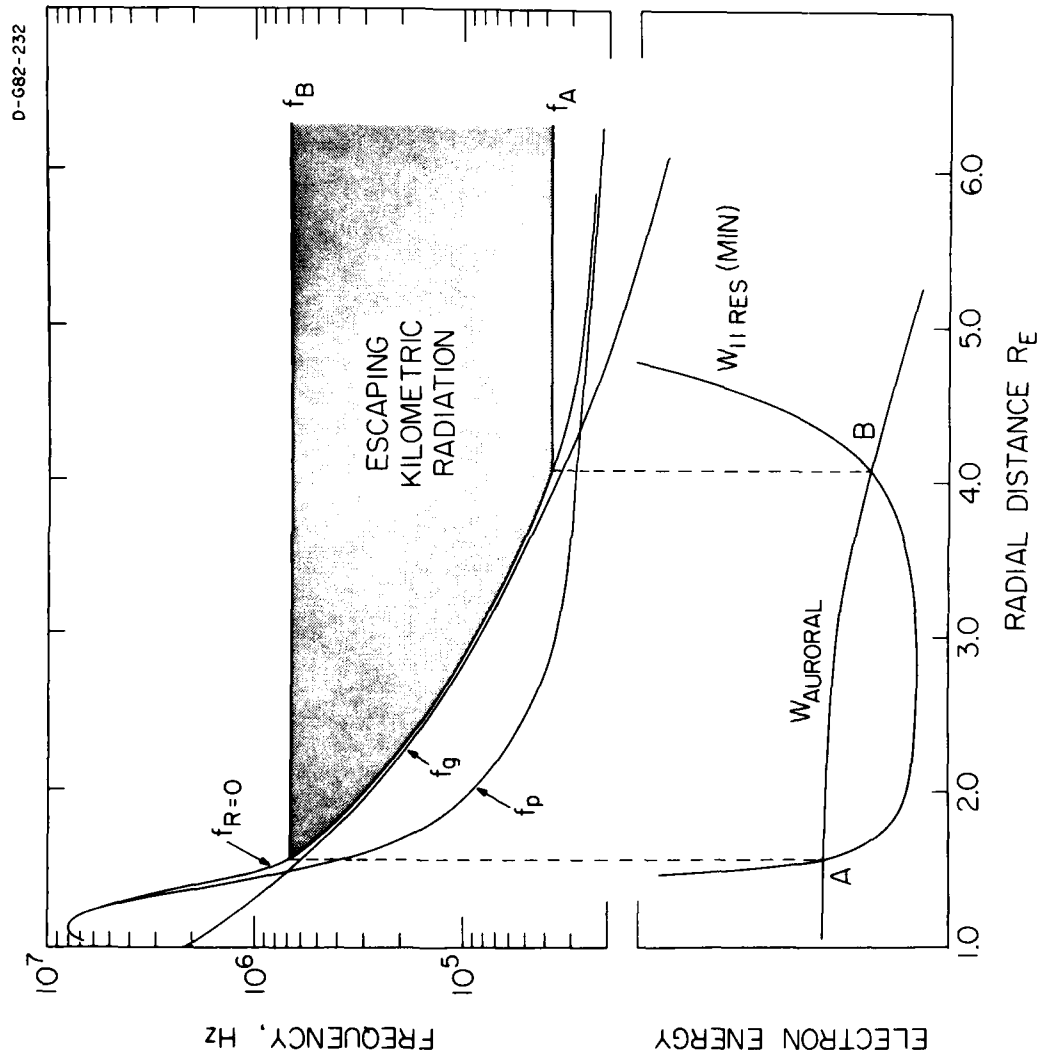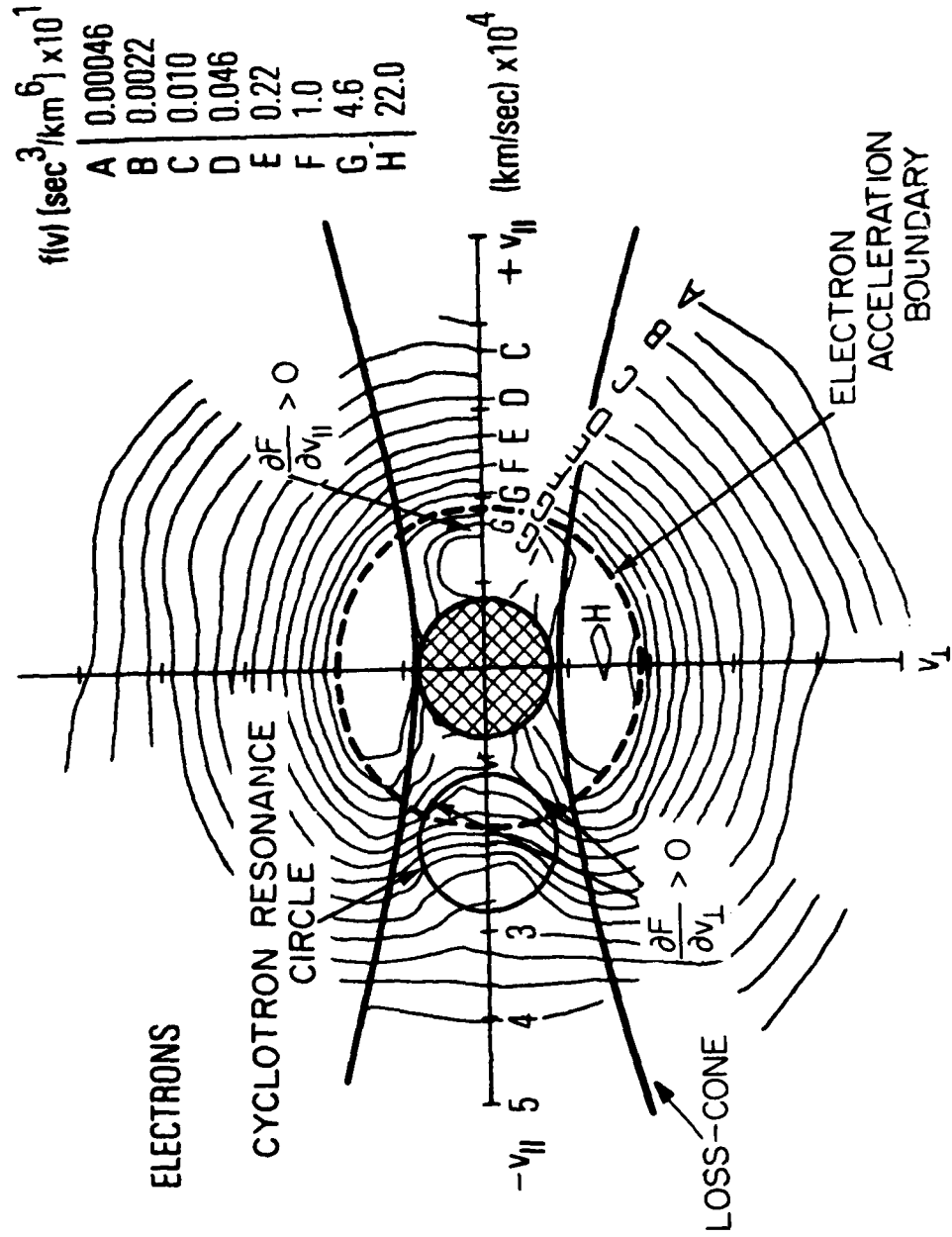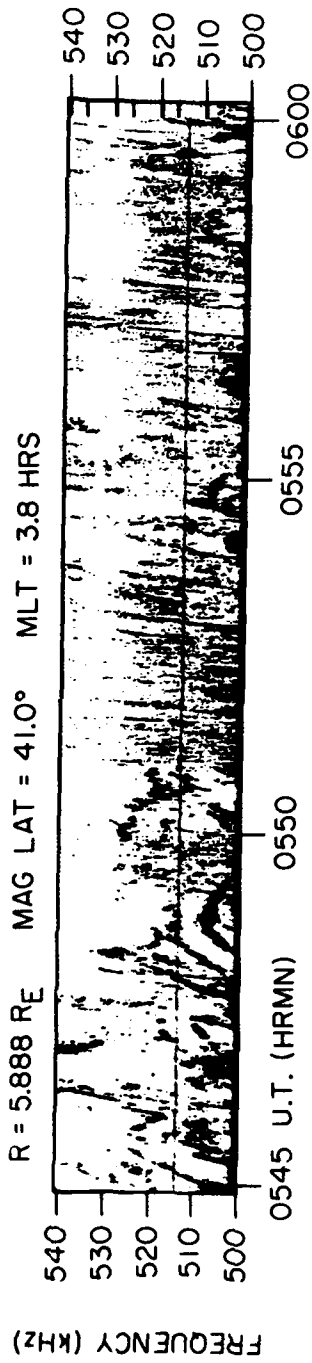
Figure 7

C-G71-68-3

INJUN 5
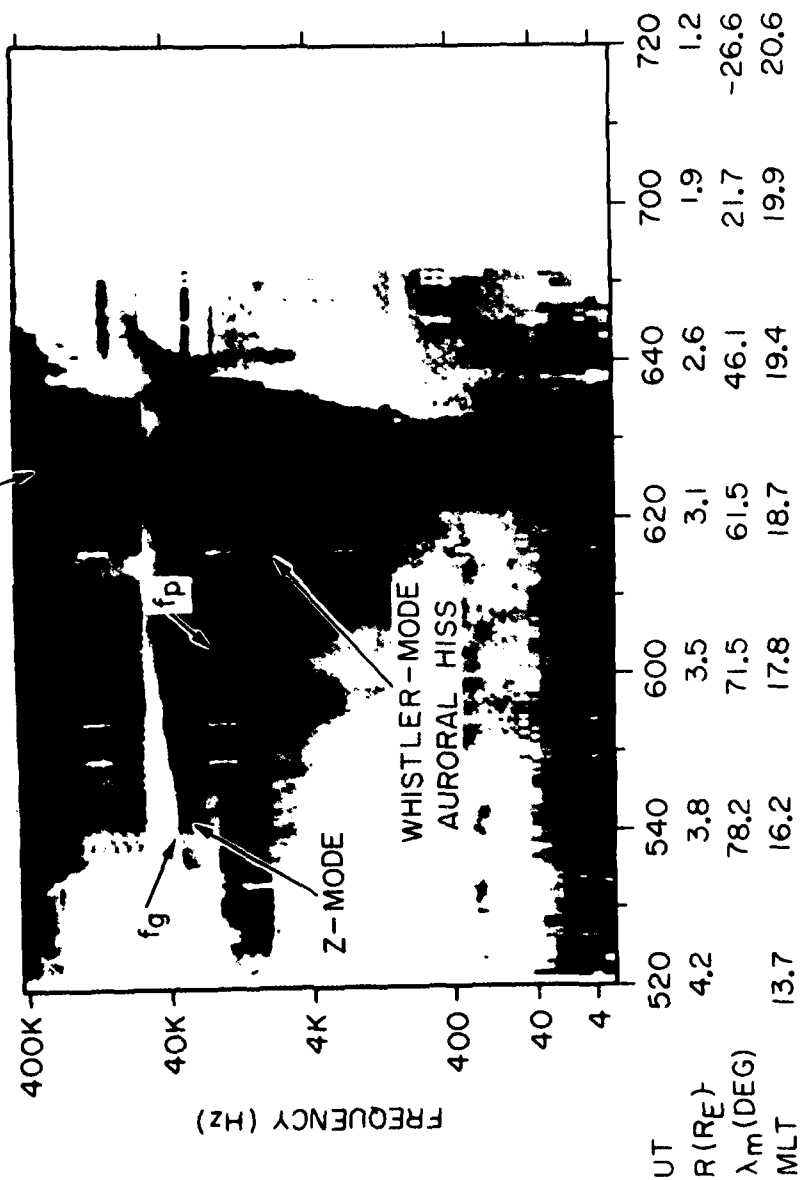**LEPEDEA 'A' ELECTRONS, REV 1403, DEC 2, 1968**
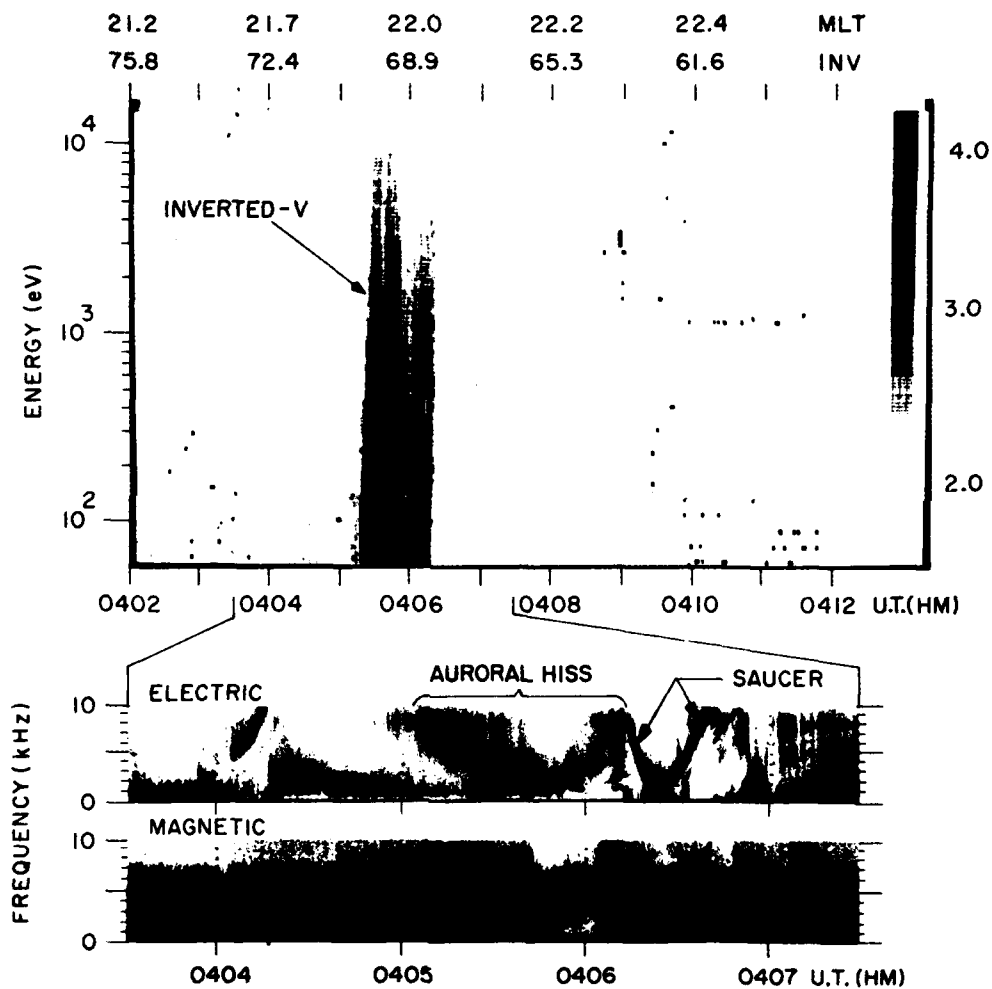
Figure 8
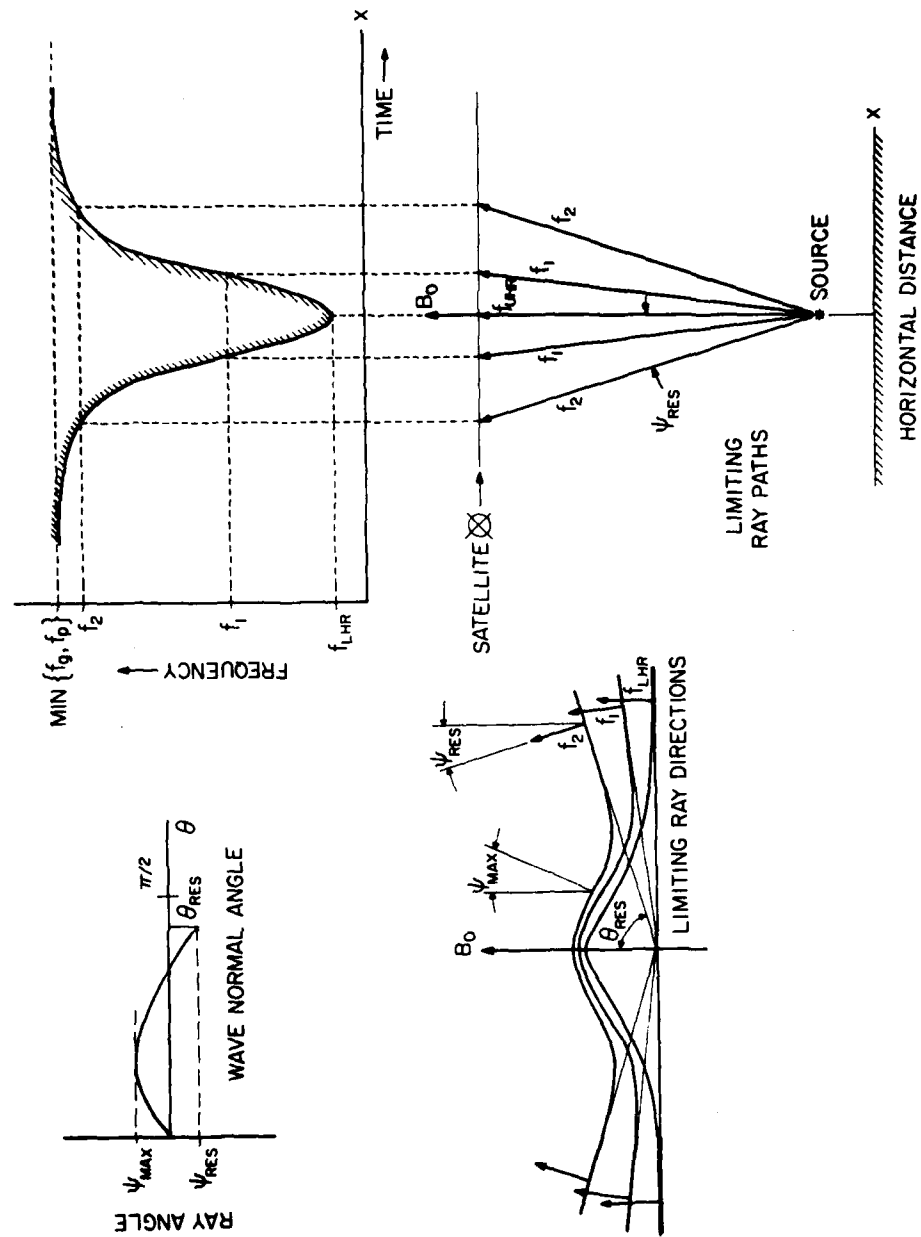
Figure 9

B-G71-140-2

Figure 10

47
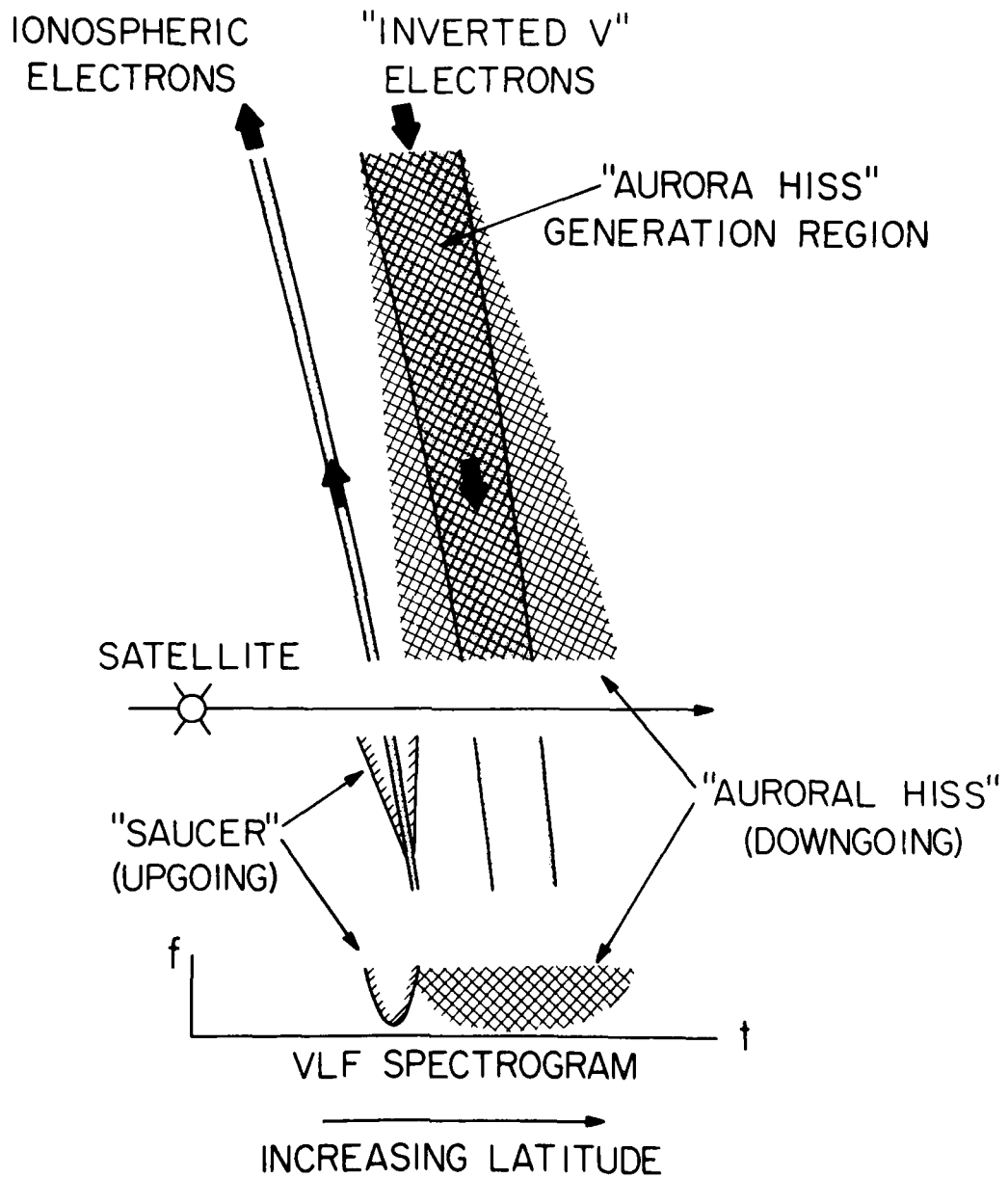
ELECTRIC FIELD, DE-1, NOVEMBER 5, DAY 309, 1981

Figure 11

A-G82-233

Figure 12